DOI: 10.1002/chem.200800175

Developing a New Class of Axial Chiral Phosphorus Ligands: Preparation and Characterization of Enantiopure Atropisomeric Phosphinines

Christian Müller,*[a] Evgeny A. Pidko,[a] Antonius J. P. M. Staring,[a] Martin Lutz,[b] Anthony L. Spek,[b] Rutger A. van Santen,[a] and Dieter Vogt[a]

Dedicated to Professor Peter Jutzi on the occasion of his 70th birthday

Abstract: Both enantiomers of the first atropisomeric phosphinine (**1**) have been isolated by using analytical HPLC on a chiral stationary phase. The enrichment of one enantiomer and a subsequent investigation into its racemization kinetics revealed a barrier for internal rotation of $\Delta G^{\neq}_{298} = (109.5 \pm 0.5)\,\mathrm{kJ\,mol^{-1}}$, which is in excellent agreement with the theoretically predicted value of $\Delta G^{\neq}_{298} = 116\,\mathrm{kJ\,mol^{-1}}$. Further analysis with UV and circular dichroism spectroscopies and density functional theory calculations led to the determination and assignment of the absolute configurations of both enantiomers. These results are the basis for future investigations into this new class of axially chiral phosphinine-based ligands and their possible applications in asymmetric homogeneous catalysis.

Keywords: atropisomerism · chirality · density functional calculations · phosphinines · phosphorus heterocycles

Introduction

λ^3-Phosphinines (also known as phosphabenzenes or phosphorins), the homologues of pyridines, have been known for more than 40 years and have a rich and versatile coordination chemistry.[1–3] However, investigations into their suitability as ligands in homogeneous catalysis only started a decade ago, and reports are limited to just a few examples.[4]

To implement fully phosphinine-based ligands in homogeneous catalysis, the availability of functionalized heterocycles and their facile modification is essential to fine-tune the stereoelectronic ligand properties and incorporate chirality for application in asymmetric reactions. We recently demonstrated the synthesis of various donor-functionalized phosphinines via a pyrylium salt intermediate, which introduced specific substituents into defined positions on the heterocyclic framework.[5] This modular approach also allowed us to design and synthesize the first atropisomeric phosphinine **1** (*R*, *S*) by enforcing restricted rotation around a C_{aryl}–$C_{aryl'}$ bond (Scheme 1).[6,7] By using density functional theory (DFT) calculations, an energy barrier for internal rotation of $\Delta G^{\neq}_{298} = 116\,\mathrm{kJ\,mol^{-1}}$ for the enantiomerization of **1** was predicted, which is expected to be high enough for configurational stability under ambient conditions.[8] Compound **1** was obtained as a racemic mixture, but we have already demonstrated that both enantiomers can be detected with

[a] Dr. C. Müller, E. A. Pidko, A. J. P. M. Staring, Prof. Dr. R. A. van Santen, Prof. Dr. D. Vogt
Department of Chemical Engineering and Chemistry
Schuit Institute of Catalysis
Eindhoven University of Technology
5600 MB Eindhoven (The Netherlands)
Fax: (+31) 402-455-054
E-mail: c.mueller@tue.nl

[b] Dr. M. Lutz, Prof. Dr. A. L. Spek
Bijvoet Center for Biomolecular Research
Crystal and Structural Chemistry
Utrecht University, Padualaan 8
3584 CH Utrecht (The Netherlands)

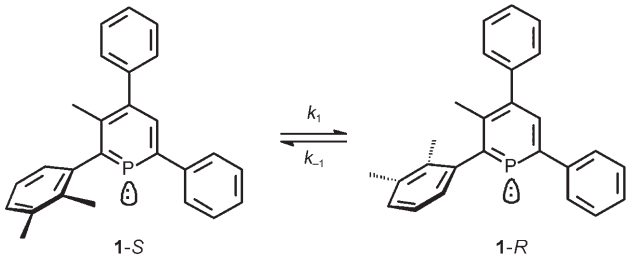

1-*S* **1**-*R*

Scheme 1. Axially chiral phosphinine **1** (*R*, *S*).

sufficient separation by using analytical HPLC on a chiral stationary phase.

Herein, we report the preparation, isolation, and characterization of enantiopure atropisomeric phosphinines **1**-*R* and **1**-*S*. Furthermore, the energy barrier for internal rotation was determined experimentally and the absolute configurations were assigned in combination with DFT calculations.

Results and Discussion

The key intermediate for the preparation of **1** is 2,3-dimethylpropiophenone (**2**; Scheme 2).[9] The use of a propiophenone, rather than an acetophenone, ultimately results in

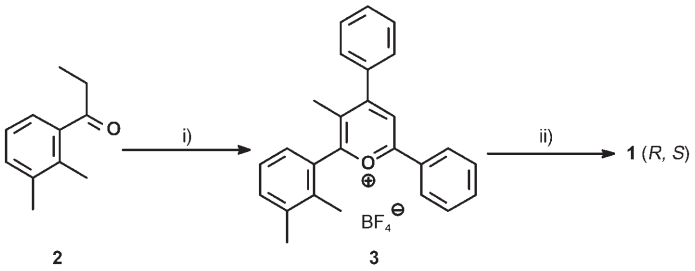

Scheme 2. Synthesis of phosphinine **1**. Reaction conditions: i) *trans*-benzylideneacetophenone (2 equiv), $HBF_4{\cdot}Et_2O$, 70 °C; ii) $P(CH_2OH)_3$, C_5H_5N, 125 °C.

the placement of a methyl group at the 3-position of the heterocycle, which is necessary to maintain the axial chirality.[10] Treatment of **2** with of *trans*-benzylideneacetophenone (2 equiv) in the presence of $HBF_4{\cdot}Et_2O$ gave pyrylium salt **3** as a racemic mixture, which was obtained as a yellow solid in moderate yield (Scheme 2).[6]

Slow evaporation of the solvent from a concentrated solution of **3** in methanol gave crystals that were suitable for X-ray diffraction. The molecular structure of **3** is illustrated in Figure 1, along with selected bond lengths and angles.

Pyrylium salt **3** crystallizes as a racemate in the centrosymmetric space group *C*2/*c*. This result not only confirms the expected substitution pattern, but also shows that the plane of the xylyl substituent in the 2-position is almost perpendicular (torsion angle = 72.9(2)°) to the plane of the heterocycle as a result of the expected restricted rotation around the C_1–C_6 bond. Thus, the molecular structure of **3** is similar to that of the first atropisomeric pyrylium salt we recently reported.[6]

Pyrylium salt **3** was further converted into the corresponding racemic phosphinine **1** by treatment with excess $P(CH_2OH)_3$[11] in pyridine at reflux (Scheme 2). After column chromatography, compound **1** was obtained as a yellow powder (34% yield) and could be isolated as yellow needles after recrystallization from hot acetonitrile or pentane. Figure 2 shows the ^1H and $^{31}P\{^1H\}$ NMR spectra of **1** in $[D_6]C_6H_6$. The $^{31}P\{^1H\}$ NMR spectrum illustrates the characteristic downfield shift of the phosphorus signal at $\delta =$ 190.6 ppm. The ^1H NMR spectrum shows a doublet at $\delta =$ 7.95 ppm with a coupling constant of $^3J(H,P) = 5.6$ Hz, which is characteristic of the P-heterocyclic proton (H_β) in an asymmetrically substituted phosphinine. The doublet at $\delta =$ 2.06 ppm with a coupling constant of $^4J(H,P) = 2.0$ Hz was assigned to the exo-heterocyclic CH_3 group and the two remaining CH_3 groups of the xylyl subsitutent were assigned to singlets at $\delta = 2.03$ and 1.98 ppm.

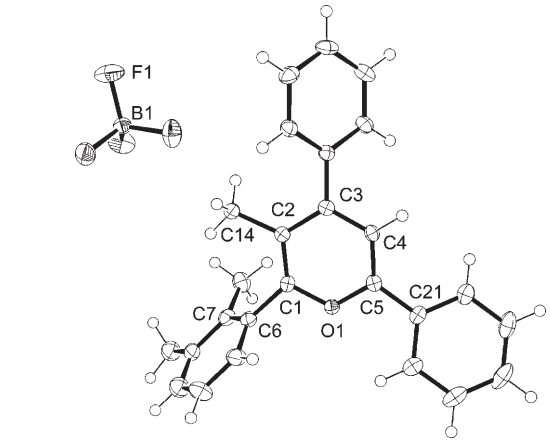

Figure 1. Molecular structure of **3** determined by X-ray crystallography. Displacement ellipsoids are shown at the 50% probability level. Selected bond lengths [Å]: C1–O1 1.3509(19), O1–C5 1.3346(19), C5–C21 1.463(2), C1–C6 1.486(2), C2–C14 1.508(2); torsion angle [°]: C7-C6-C1-C2 72.9(2).

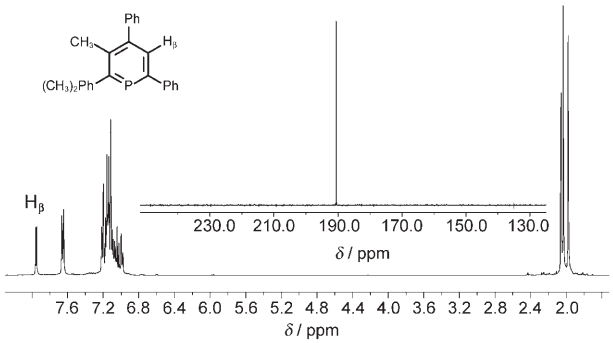

Figure 2. ^1H NMR (400 MHz, $[D_6]C_6H_6$) spectrum of **1**. Inset: $^{31}P\{^1H\}$ NMR (162 MHz, $[D_6]C_6H_6$) spectrum of **1**.

A very good separation of enantiomers **1**-E_1 (eluted first) and **1**-E_2 (eluted second) was achieved by using analytical HPLC on a chiral stationary phase with *n*-hexane as the eluent (Chiralcel OD-H, $t_1 = 17.75$ min, $t_2 = 22.98$ min, 25 °C, flow rate 1 mL min^{-1}). HPLC analysis of both fractions with the same chiral column revealed that both isomers could be obtained with an enantiopurity of 99%. Additionally, the successful separation of the enantiomers confirmed our original assumption that the energy barrier for internal rotation is reasonably high (Figure 3).

Isolation of the enantiomers also provided an opportunity to determine the energy barrier for internal rotation experi-

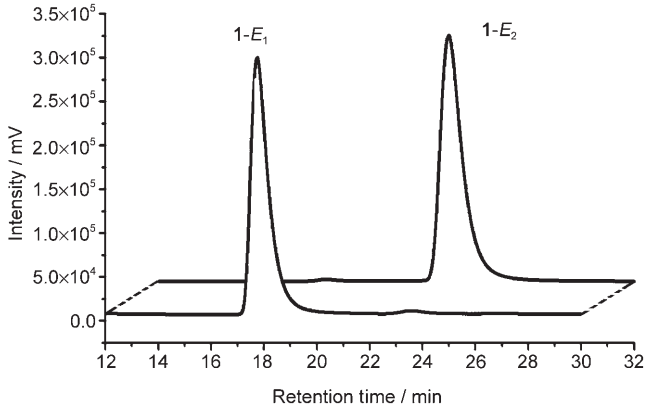

Figure 3. A chromatogram of **1**-E_1 and **1**-E_2 after HPLC separation of racemic **1**.

mentally. The thermal racemization at constant temperature of preparatively enriched **1**-E_1 was followed over regular time intervals and over at least two half-lives (Figure 4).[12] The results show that a ratio of **1**-E_1/**1**-E_2 of 59:41 was reached after 23 d at 25 °C, which corresponds to an enantiomeric excess (*ee*) of 18 % for **1**-E_1.

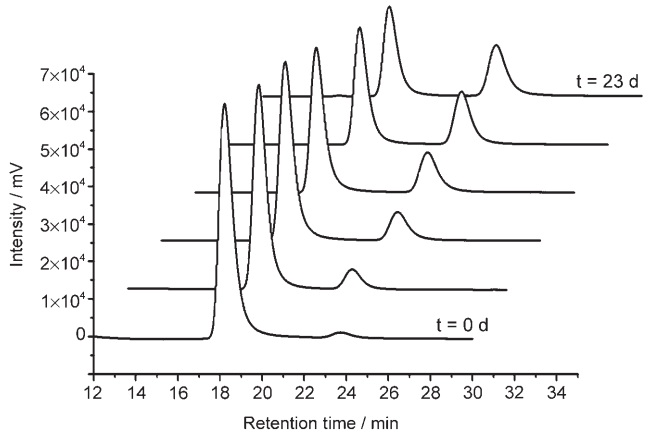

Figure 4. HPLC chromatograms of the thermal racemization of **1**-E_1 in hexane at 298 K.

The rate constant for enantiomerization ($k_1 = k_{-1}$) was determined by using reversible first-order kinetics for the interconverison of enantiomers **1**-E_1 and **1**-E_2 (see also Scheme 1) according to Equation (1):

$$\ln\left(\frac{[M]_t - [M]_{eq}}{[M]_0 - [M]_{eq}}\right) = -2kt \qquad (1)$$

in which $[M]_t$ is the molar concentration at time t, $[M]_0$ is the initial molar concentration, and $[M]_{eq}$ is the equilibrium molar concentration of one enantiomer. Alternatively, we used the corresponding percentage values of the enantiomers obtained from the HPLC analysis described above (Figure 4), with $[M]_{eq} = 50\,\%$.

Plotting $-\ln([M]_t - [M]_{eq}/[M]_0 - [M]_{eq})$ versus time for **1**-E_2 gave a value of $k_1 = k_{-1} = (4.2 \pm 0.8) \times 10^{-7}\ s^{-1}$ at 298 K (Figure 5). Thus, a value of $\Delta G^{\neq}_{298} = (109.5 \pm 0.5)\ kJ\,mol^{-1}$ for

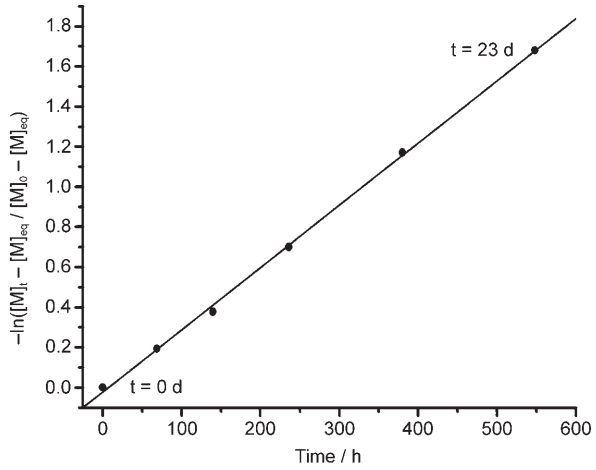

Figure 5. Plot of $-\ln([M]_t - [M]_{eq}/[M]_0 - [M]_{eq})$ versus time at 298 K for **1**-E_2.

the free activation energy and a value of $\tau = t_{1/2} = (9.6 \pm 2.1)$ d for the half-life were determined by using the Eyring equation [Eq. (2)] and Equation (3) to calculate the reversible first-order kinetics for the interconversion of **1**-E_1 and **1**-E_2 (see also Table 1).[13,14]

$$\Delta G^{\neq} = RT\ln\left(\frac{k_B T}{kh}\right) \qquad (2)$$

$$\tau = t_{1/2} = \frac{\ln 2}{(2k)} \qquad (3)$$

Table 1. Experimentally and theoretically determined kinetic parameters for phosphinine **1**.[14]

		$\Delta G^{\neq}_{298}$ [kJ mol^{-1}]		
	$k \times 10^{-7}$ [s^{-1}]	Exptl[a]	Calcd[b]	$\tau_{1/2}$ [d]
1	4.2 ± 0.8	109.5 ± 0.5	116	9.6 ± 2.1

[a] Experimentally obtained value. Conditions: hexane, $T = 298$ K. [b] Value obtained from DFT calculations with B3LYP/6-31G(d,p).

The experimentally determined value of $\Delta G^{\neq}_{298}$ for the energy barrier for internal rotation agrees well with the value calculated by using DFT ($\Delta G^{\neq}_{298} = 116\ kJ\,mol^{-1}$).[6] These results also show, however suggest that configurational stability is not guaranteed at higher temperatures, and thus, under typical catalytic reaction conditions, although the situation in the corresponding metal complexes might be considerably different and higher free activation energies for the interconversion of the enantiomers are expected. Nevertheless, it demonstrates that theoretical calculations are powerful tools for predicting and estimating physical organic properties of such systems and can help to design suitable ligand systems prior to synthetic work.

We were also interested in the possibility of assigning the absolute configurations of **1**-E_1 and **1**-E_2. For this purpose, the optical properties of the separated enantiomers were investigated; the experimentally recorded circular dichroism (CD) and UV spectra of **1**-E_1 and **1**-E_2 in hexane are shown in Figure 6a and b. The UV absorption spectra (Figure 6b) show a shoulder at $\lambda = 300$ nm, followed by an absorption maximum at $\lambda_{max} \approx 260$ nm. These data are typical for 2,4,6-substituted triarylphosphinines in methanol (2,4,6-triphenylphosphinine: $\lambda_{max} = 278$ nm, $\lambda = 314$ nm (sh); 2,4,6-triphenylpyridine: $\lambda_{max} = 254$ nm, $\lambda = 312$ nm (sh); 2,4,6-triphenylbenzene: $\lambda_{max} = 254$ nm). These bands were originally assigned to an n→π* transition (long-wave absorption shoulder) and a π→π* ^{1}L(a) transition (short-wave absorption).[15,16] However, note that the lone pair located on the phosphorus atom is not the HOMO, and therefore, it is expected to be relatively low in energy.[15] The CD spectra (Figure 6a) show an exciton split couplet with relatively small values of $\Sigma\Delta\varepsilon \approx 15$ and ≈ 25 for **1**-E_1 and **1**-E_2, respectively, and also two Cotton effects for each enantiomer at $\lambda \approx 275$ and ≈ 210 nm. Note that as a result of the enrichment procedure, the concentrations of the enantiomers are slightly different; this can be observed in the UV spectra and may have given rise to the slight anomaly observed in the values of $\Sigma\Delta\varepsilon$.

To deduce the absolute configuration of both enantiomers, the respective CD and UV spectra were simulated by means of a time-dependent DFT method at the TD-B3LYP/6-31G(d,p) level. This technique has been shown to provide a reasonably accurate description of the photophysical properties of various compounds, which includes quite accurate predictions of CD spectra.[17] We optimized the geometries of **1**-*R* and **1**-*S* (see Scheme 1) at the B3LYP/6-31G(d,p) level and calculated their theoretical CD and UV spectra, which are shown in Figure 6c and d, respectively.

It can be seen that the theoretical UV spectrum (Figure 6d) has the same qualitative features as those observed in the experimental spectrum (Figure 6b). Moreover, the positioning of the bands in both cases is very similar. Analysis of the calculated electronic absorption bands also reveals that the shoulder at $\lambda \approx 300$ nm should in fact be attributed to π→π* transitions, with major contributions from HOMO→LUMO and HOMO^{-1}→LUMO excitations. The absorption maximum at $\lambda_{max} \approx 260$ nm, on the other hand, was attributed to a combination of π→π* and n→π* transi-

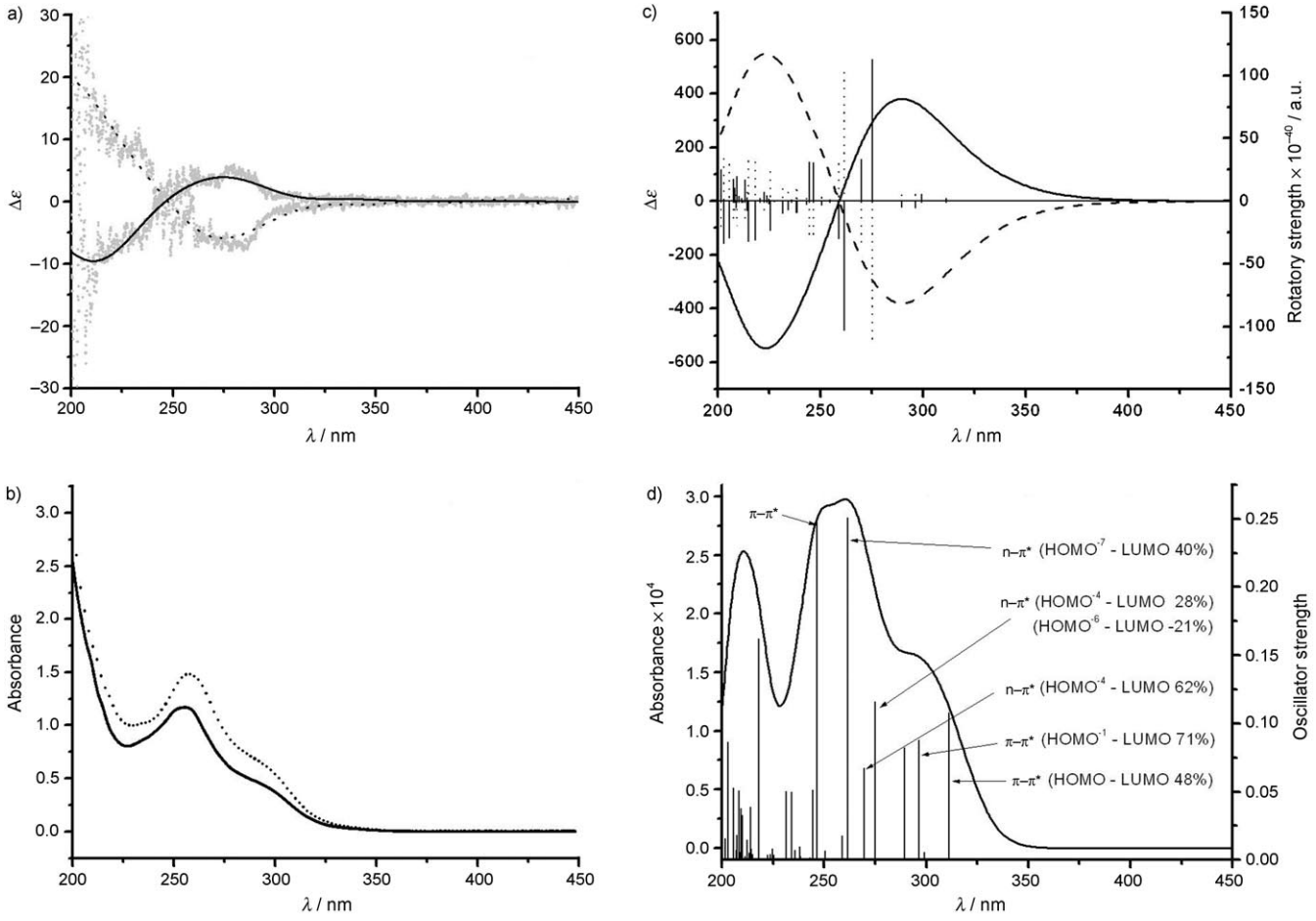

Figure 6. Experimental CD (a) and UV (b) spectra of **1**-E_1 (——) and **1**-E_2 (•••••) in hexane. The experimental CD spectra (gray lines) have been smoothed (black lines) to reduce the high noise level. Theoretical CD (c) and UV (d) spectra of enantiomers **1**-*R* (– – –) and **1**-*S* (——).

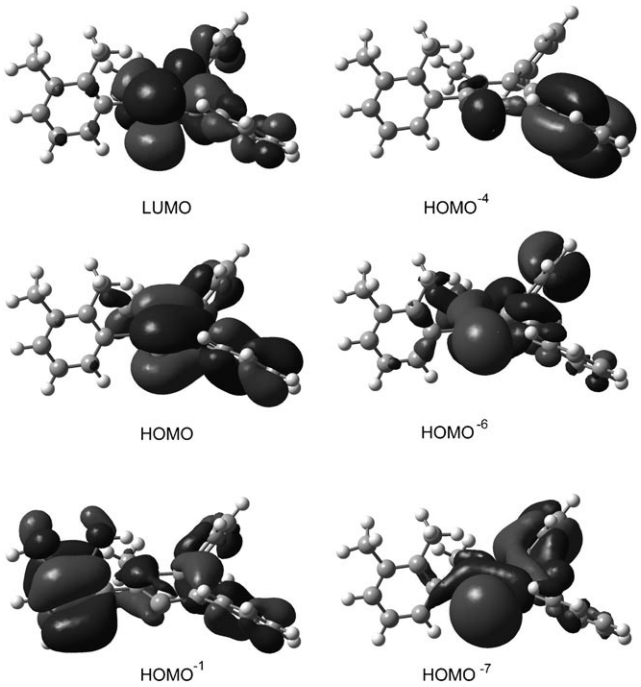

Figure 7. FMOs of phosphinine **1**.

tions (see Figure 6d). The respective frontier molecular orbitals (FMOs) are depicted in Figure 7.

The theoretical CD spectra (Figure 6c) of both enantiomers reproduce well the features of those obtained experimentally (Figure 6a), in particular, the bisignate shape as well as the sequence and positions of the negative/positive Cotton effects. However, the intensity maxima of the theoretical spectra match less well and are, in general, larger than those of the experimental spectra. Note that, even though the rotation of the phenyl groups at the 4- and 6-positions on the heterocycle does have an influence on the shape of the theoretical CD spectrum, the theoretically predicted and experimentally observed bisignate nature of the spectra remains unchanged and is independent of the conformations of these phenyl substituents.

The qualitative agreement between the experimental results and the theoretical calculations allowed us to unambiguously assign the **1**-*S* configuration to **1**-E_1 and the **1**-*R* configuration to **1**-E_2, as illustrated in Figure 8.

Conclusion

We have demonstrated the successful separation of enantiomers of the first axially chiral phosphinine **1** by means of analytical HPLC on a chiral stationary phase. The atropisomers were isolated with an enantiopurity of 99% and an energy barrier for internal rotation of $\Delta G^{\ddagger}_{298} = (109.5 \pm 0.5)\ \mathrm{kJ\,mol^{-1}}$ was experimentally determined by thermal racemization and showed a very good agreement with the theoretically predicted value of $\Delta G^{\ddagger}_{298} = 116\ \mathrm{kJ\,mol^{-1}}$. The assignment of the absolute configurations **1**-*R* and **1**-*S* was achieved by comparing the experimental CD spectra of both enantiomers with theoretical spectra from optimized structures. Investigations on ligands with different substitution patterns and higher rotational energy barriers are currently in progress. Their separation on a preparative scale and the influence of metal coordination on the free energy of activation for the interconversion of enantiomers are being investigated. These properties are of particular interest because configurational stability at higher temperature, and thus under typical catalytic reaction conditions, is a prerequisite for the successful application of this new class of axially chiral phosphorus-containing ligands in asymmetric homogeneous catalysis. The results presented herein provide the basis for future investigations in this research area.

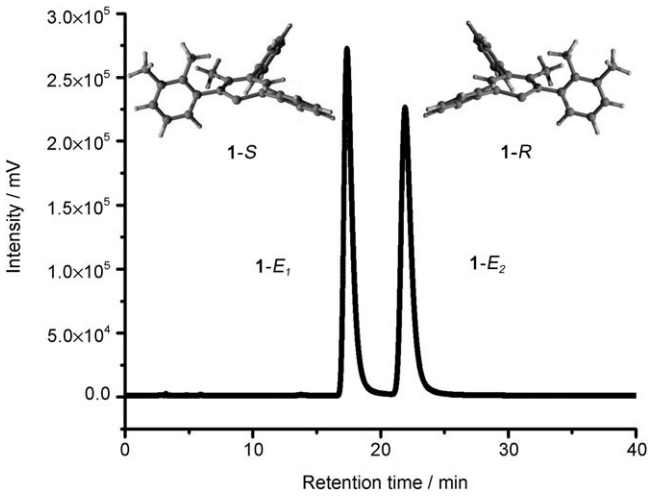

Figure 8. HPLC analysis of **1** and assignment of the absolute configurations: **1**-E_1 = **1**-*S*, **1**-E_2 = **1**-*R*.

Experimental Section

General: The ^{1}H and ^{31}P{^{1}H} NMR spectra were recorded by using a Varian Mercury 400 spectrometer. HPLC analysis and fraction collection was performed by using HPLC equipment that consisted of a Shimadzu LC-20 AD pump, a Shimadzu SPD-20 A UV/Vis detector, a Spark Holland Marathon autosampler, a homemade oven with a column selector, and an LKB 2211 Superrac fraction collector. Column and analysis specifications: Chiralcel OD-H (250×4.6 mm, particle size: 5 μm, purchased from Daicel), eluent = *n*-hexane, column temperature = 25 °C, flow rate = 1 mL min^{-1}, pressure = 34 bar, λ = 254 nm (UV detector), injection volume = 20 μL.

Enrichment and determination of racemization kinetics of 1-E_1: Phosphinine **1** was prepared according to a previously reported procedure[6] and recrystallized from hot, degassed, dry acetonitrile to give **1** as bright yellow needles. Racemate **1** (1 mg, 8.2×10^{-6} mol) was dissolved in degassed *n*-hexane (1 mL), prior to HPLC enrichment. Enantiomer **1**-E_1 was eluted and collected under an argon atmosphere and the solvent was evaporated. This procedure was performed twelve times, and the combined residues of **1**-E_1 were redissolved in degassed *n*-hexane (6.0 mL) to give a final concentration of approximately 1×10^{-4} M. This solution was stirred at 25 °C and aliquots (0.7 mL) were analyzed by using HPLC at time intervals of t = 0, 3, 6, 10, 16, and 23 d.

UV and CD analysis: UV/Vis and CD spectroscopic measurements were performed at 25 °C by using a Jasco J-815 spectropolarimeter. Appropriate settings were chosen for the sensitivity, time constant, and scan rate and 0.1 cm cuvettes were used.

Racemate **1** (3 mg, 2.7×10^{-6} mol) was dissolved in degassed *n*-hexane (1 mL), prior to HPLC separation. Enantiomers **1**-E_1 and **1**-E_2 were eluted and collected under an argon atmosphere and the solvent was evaporated. This procedure was performed three times and the combined residues of **1**-E_1 and **1**-E_2 were each redissolved in degassed hexane (0.6 mL) to give final concentrations of approximately $2.7\cdot10^{-4}$ M. The UV and CD spectra were recorded immediately.

X-ray crystal structure determination of 3: Crystals suitable for X-ray diffraction were obtained by slow evaporation of the solvent from a concentrated solution of **3** in methanol.

Crystallographic data: $C_{26}H_{23}O\cdot BF_4$; $M_r=438.25$; yellow block; $0.37\times0.27\times0.22$ mm^3; monoclinic; *C*2/*c* (no. 15); $a=35.478(3)$, $b=7.7312(5)$, $c=15.8455(11)$ Å; $\beta=99.877(2)°$; $V=4281.9(2)$ Å^3; $Z=8$; $\rho=1.360$ g cm^{-3}; $\mu=0.104$ mm^{-1}. 37 605 reflections were measured by using a Nonius Kappa CCD diffractometer with a rotating anode (graphite monochromator, $\lambda=0.71073$ Å) up to a resolution of $(\sin\theta/\lambda)_{max}=0.61$ Å^{-1} at a temperature of 150 K. The reflections were corrected for absorption and scaled on the basis of multiple measured reflections by using the SADABS program[18] (0.70–0.97 correction range). 3987 reflections were unique ($R_{int}=0.027$). The structures were solved with SHELXS-97[19] by using direct methods and refined with SHELXL-97[19] on F^2 for all reflections. Non-hydrogen atoms were refined by using anisotropic displacement parameters. All hydrogen atoms were located by using difference Fourier maps and refined with a riding model. 292 parameters were refined with no restraints. R_1/wR_2 [$I>2\sigma(I)$]: 0.0404/0.0973, R_1/wR_2 (all reflns): 0.0503/0.1030, $S=1.042$, residual electron density was between −0.28 and 0.55 e Å^{-3}. Geometry calculations and checks for higher symmetry were performed with the PLATON program.[20]

CCDC-675769 (**3**) contains the supplementary crystallographic data for this paper. These data can be obtained free of charge from The Cambridge Crystallographic Data Centre via www.ccdc.cam.ac.uk/data_request/cif.

Computational details: Quantum chemical calculations were carried out with DFT by using the Gaussian 03[21] program at the B3LYP/6-31G(d,p) level. Full geometry optimizations were performed for compounds **1**-*R*, **1**-*S*, and the transition state of racemization. The nature of the stationary points was tested by analyzing the analytically calculated harmonic normal modes. The local minimum structures did not show imaginary frequencies, whereas the transition-state structure showed a single imaginary frequency that corresponded to an eigenvector along the reaction path, that is, internal rotation about the C_{aryl}–$C_{aryl'}$ bond. The theoretical UV/Vis spectra were calculated at the same level as the geometry optimizations, by using the time-dependent DFT method that is implemented in the Gaussian 03 program package.[21] To simulate absorption spectra, the full width at half-maximum of the gaussian curves used to generate the spectra was set to 3000 cm^{-1}. The CD spectra were simulated with the assumption that the bandwidth at 1/e of the height of the gaussian curves used to generate the spectrum was equal to 1 eV.

Acknowledgements

The authors would like to thank Dr. Subi Jacob George (TU/e, Laboratory of Macromolecular Chemistry) for recording the CD and UV spectra and Joost van Dongen for valuable advice on HPLC analysis. This work was supported in part (ML, ALS) by the Council for the Chemical Sciences of the Netherlands Organization for Scientific Research (CW-NWO).

[1] a) G. Märkl, *Angew. Chem.* **1966**, *78*, 907–908; *Angew. Chem. Int. Ed. Engl.* **1966**, *5*, 846–847.; b) A. J. Ashe III, *J. Am. Chem. Soc.* **1971**, *93*, 3293–3295.

[2] For recent reviews, see: a) C. Müller, D. Vogt, *Dalton Trans.* **2007**, 5505–5523; b) P. Le Floch, *Coord. Chem. Rev.* **2006**, *250*, 627–681; c) F. Mathey, P. Le Floch, *Science of Synthesis* **2005**, *15*, 1097–1155; d) F. Mathey, *Angew. Chem.* **2003**, *115*, 1616–1643; *Angew. Chem. Int. Ed.* **2003**, *42*, 1578–1604; e) P. Le Floch, F. Mathey, *Coord. Chem. Rev.* **1998**, *179–180*, 771–791.

[3] a) P. Le Floch in *Phosphorus–Carbon Heterocyclic Chemistry: The Rise of a New Domain*, (Ed.: F. Mathey), Pergamon, Palaiseau, **2001**, pp. 485–533; b) G. Märkl in *Multiple Bonds and Low Coordination in Phosphorus Chemistry*, (Eds.: M. Regitz, O. J. Scherer), Thieme, Stuttgart, **1990**, p. 220.

[4] a) F. Knoch, F. Kremer, U. Schmidt, U. Zenneck, P. Le Floch, F. Mathey, *Organometallics* **1996**, *15*, 2713–2719; b) B. Breit, *Chem. Commun.* **1996**, 2071–2072; c) B. Breit, *J. Mol. Catal. A* **1999**, *143*, 143–154; d) B. Breit, R. Winde, K. Harms, *J. Chem. Soc. Perkin Trans. 1* **1997**, *18*, 2681–2682; e) B. Breit, R. Winde, T. Mackewitz, R. Paciello, K. Harms, *Chem. Eur. J.* **2001**, *7*, 3106–3121; f) L. Weber, *Angew. Chem.* **2002**, *114*, 583–592; *Angew. Chem. Int. Ed.* **2002**, *41*, 563–572; g) M. T. Reetz, G. Mehler, *Tetrahedron Lett.* **2003**, *44*, 4593–4596; h) M. T. Reetz, X. Li, *Angew. Chem.* **2005**, *117*, 3022–3024; *Angew. Chem. Int. Ed.* **2005**, *44*, 2962–2964; i) C. Müller, L. Guarrotxena-Lopéz, H. Kooijman, A. L. Spek, D. Vogt, *Tetrahedron Lett.* **2006**, *47*, 2017–2020.

[5] a) C. Müller, M. Lutz, A. L. Spek, D. Vogt, *J. Chem. Crystallogr.* **2006**, *36(12)*, 869–874; b) C. Müller, D. Wasserberg, J. J. M. Weemers, E. A. Pidko, S. Hoffmann, M. Lutz, A. L. Spek, S. C. J. Meskers, R. A. J. Janssen, R. A. van Santen, D. Vogt, *Chem. Eur. J.* **2007**, *13*, 4548–4559; c) C. Müller, Z. Freixa, M. Lutz, A. L. Spek, D. Vogt, P. W. N. M. van Leeuwen, *Organometallics* **2008**, *27*, 834–838.

[6] C. Müller, E. A. Pidko, M. Lutz, A. L. Spek, R. A. van Santen, D. Vogt, *Dalton Trans.* **2007**, 5372–5375.

[7] For related atropisomeric pyridines, see: a) A. Gutnov, B. Heller, C. Fischer, H.-J. Drexler, A. Spannenberg, B. Sundermann, C. Sundermann, *Angew. Chem.* **2004**, *116*, 3883–3886; *Angew. Chem. Int. Ed.* **2004**, *43*, 3795–3797; b) B. Heller, A. Gutnov, C. Fischer, H.-J. Drexler, A. Spannenberg, D. Redkin, C. Sundermann, B. Sundermann, *Chem. Eur. J.* **2007**, *13*, 1117–1128.

[8] G. Bringmann, A. J. Price Mortimer, P. A. Keller, M. J. Gresser, J. Garner, M. Breuning, *Angew. Chem.* **2005**, *117*, 5518–5563; *Angew. Chem. Int. Ed.* **2005**, *44*, 5384–5427.

[9] A. Shiozawa, K. Narita, G. Izumi, S. Kurashige, K. Sakitama, M. Ishikawa, *Eur. J. Med. Chem.* **1995**, *30*, 85–94.

[10] S. M. M. Elshafie, *J. Prakt. Chemie* **1982**, *324*, 149–154.

[11] J. W. Ellis, K. N. Harrison, P. A. T. Hoye, A. G. Orpen, P. G. Pringle, M. B. Smith, *Inorg. Chem.* **1992**, *31*, 3026–3033.

[12] a) S. Funda Oğuz, İ. Doğan, *Tetrahedron: Asymmetry* **2003**, *14*, 1857–1864; b) M. T. Harju, P. Haglund, *Fresenius J. Anal. Chem.* **1999**, *364*, 219–223.

[13] a) K. Cabrera, M. Jung, M. Fluck, V. Schurig, *J. Chromatogr. A* **1996**, *731*, 315–321; b) R. J. Friary, M. Spangler, R. Osterman, L. Schulman, J. H. Schwerdt, *Chirality* **1996**, *8*, 364–371.

[14] The errors for k, ΔG, and τ were determined by assuming an estimated error of 1% for the integrated areas of the HPLC chromatogram.

[15] K. Dimroth, *Fortschr. Chem. Forsch.* **1973**, *38*, 1–147.

[16] G. Märkl, *20 Jahre Fonds der Chemischen Industrie*, Verband der Chemischen Industrie, Frankfurt, **1970**, p. 113.

[17] a) *Circular Dichroism: Principles and Applications*, (Eds.: K. Nakanishi, N. Berova, R. W. Woody), VCH, Weinheim, **1994**; b) D. Casarini, L. Lunazzi, M. Mancinelli, A. Mazzanti, C. Rosini, *J. Org. Chem.* **2007**, *72*, 7667–7676; c) T. Mori, Y. Inoue, S. Grimme, *J. Phys. Chem. A* **2007**, *111*, 4222–4234; d) F. Ceccacci, G. Mancini, P. Mencarelli, C. Villani, *Tetrahedron: Asymmetry* **2003**, *14*, 3117–3122; e) N. Harada, A. Saito, N. Koumura, H. Uda, B. de Lange, W. F. Jager, H. Wynberg, B. L. Feringa, *J. Am. Chem. Soc.* **1997**, *119*, 7241–7248.

[18] G. M. Sheldrick, *SADABS: Area-Detector Absorption Correction*, v2.10, Universität Göttingen, Göttingen (Germany), **1999**.

[19] G. M. Sheldrick, *Acta Cryst.* **2008**, *A64*, 112–122.

[20] A. L. Spek, *J. Appl. Crystallogr.* **2003**, *36*, 7–13.
[21] Gaussian 03, Revision B.05, M. J. Frisch, G. W. Trucks, H. B. Schlegel, G. E. Scuseria, M. A. Robb, J. R. Cheeseman, J. A. Montgomery, Jr., T. Vreven, K. N. Kudin, J. C. Burant, J. M. Millam, S. S. Iyengar, J. Tomasi, V. Barone, B. Mennucci, M. Cossi, G. Scalmani, N. Rega, G. A. Petersson, H. Nakatsuji, M. Hada, M. Ehara, K. Toyota, R. Fukuda, J. Hasegawa, M. Ishida, T. Nakajima, Y. Honda, O. Kitao, H. Nakai, M. Klene, X. Li, J. E. Knox, H. P. Hratchian, J. B. Cross, V. Bakken, C. Adamo, J. Jaramillo, R. Gomperts, R. E. Stratmann, O. Yazyev, A. J. Austin, R. Cammi, C. Pomelli, J. W. Ochterski, P. Y. Ayala, K. Morokuma, G. A. Voth, P. Salvador, J. J. Dannenberg, V. G. Zakrzewski, S. Dapprich, A. D. Daniels, M. C. Strain, O. Farkas, D. K. Malick, A. D. Rabuck, K. Raghavachari, J. B. Foresman, J. V. Ortiz, Q. Cui, A. G. Baboul, S. Clifford, J. Cioslowski, B. B. Stefanov, G. Liu, A. Liashenko, P. Piskorz, I. Komaromi, R. L. Martin, D. J. Fox, T. Keith, M. A. Al-Laham, C. Y. Peng, A. Nanayakkara, M. Challacombe, P. M. W. Gill, B. Johnson, W. Chen, M. W. Wong, C. Gonzalez, J. A. Pople, Gaussian, Inc., Wallingford CT, **2004**.

Received: January 28, 2008
Published online: April 9, 2008

